Zhang, H., Brown, L. and Blunt, Liam

Investigation of characteristics at the stem cement interface in total hip replacement

INVESTIGATION OF CHARACTERISTICS AT THE STEM CEMENT INTERFACE IN TOTAL HIP REPLACEMENT

H. Zhang, L. Brown and L. Blunt
University of Huddersfield, Queensgate, Huddersfield, HD1 3DH, UK

ABSTRACT

Aseptic loosening at the stem cement interface has been noted as a prominent failure mode in cemented total hip replacement. It can be attributed to a tissue reaction to particulate debris generated by wear of the components. Wear can occur not only at the articulating surface but also at other load bearing interfaces due to relative micromotion. The stem cement interface has been consistently cited as a weak link. In the present study, characteristics at this interface were investigated through a series of pull out tests and a fretting wear simulation. The static shear strength was compared across a range of commercially available bone cements, with the result being higher than other studies. Fretting wear was successfully reproduced in vitro, which complied well with retrieval investigations. The research has gained a deep insight into the characteristics at the stem cement interface.

Keywords: stem cement interface, pull out test, fretting wear simulation

1 INTRODUCTION

Total hip replacement (THR) is one of the most common and effective procedures performed in the UK and worldwide, with the purpose of dramatically improving quality of life of patients suffering from femoral disease [1]. THR involves securing a prosthetic head by the insertion of a femoral stem into a cavity in the femur, relying on either an uncemented method which depends on bone ingrowth into the porous coating on the stem surface for fixation, or more commonly a cemented method which utilises polymethylmethacrylate (PMMA) bone cement for fixation. With an increasing prevalence of this procedure performed in younger people coupled with a longer life expectancy, it is hoped that this total joint system could function well for at least 15-20 years. However, up to 10% of the 50,000 operations carried out annually are to revise prostheses which have failed prematurely. Great efforts have been made to gain an insight into the failure scenario behind cemented THR, and aseptic loosening has nowadays been generally accepted as the primary cause, which dominates mechanical malfunctioning of the joint system. It can be attributed to a tissue reaction to particulate debris generated by wear of the components. Wear can occur not only at the articulating surface but also at other load bearing interfaces. It is now considered that wear at the stem cement interface shows an increasing significance in the overall wear of cemented THR, and much research has been performed [2-4]. However, the mechanical aspects of stem loosening have not been fully understood. It is therefore required to gain a further insight into the characteristics at the stem cement interface. This present study seeks to address this issue by carrying out a series of pull out tests, with the aim of obtaining the static shear strength between a polished femoral stem and several commercially available bone cements, which is considered to contribute significantly to early debonding at the stem cement interface. Additionally, an in vitro simulation has been performed, intending to reproduce fretting wear successfully and gain a better understanding of the wear mechanism involved in cemented THR.

2 PULL OUT TEST

The static shear strength between a polished femoral stem and seven commercially available bone cements were investigated through pull out tests. The details of the cements are shown in table 1. Stainless steel rods, 12mm in diameter and 55mm long, were manufactured for each cement type. These rods were then polished to obtain a surface roughness value of Sq~10nm, measured by a Wyko NT 2000 interferometer at x50 magnification, this roughness being directly comparable to a polished Exeter stem. A cylindrical holder made of mild steel was fabricated for the bone cement to be poured into, leaving a cement mantle thickness of 7mm. The metallic rod was fixed using a milling machine chuck, which ensured accurate axial alignment of the rod within the cement mantle. The cements were all hand mixed at room temperature, according to the manufactures' instructions. The specimen was laid aside for 24 hours to fully cure before being tested on a Hounsfield Test Machine H20K-W. All the tests were performed at a constant speed of 2mm/min by displacement control, and a load-displacement plot was recorded. Repeated testes were carried out five times to provide statistical viability. After each test, the stainless steel rod was repolished and the cement was cut longitudinally into two equal parts following extraction from the holder. The inner surface of bone cement was cleaned with alcohol and stained using red dye, enabling observation of porosity with a Leica optical microscope MZ6. In total 10 images were taken arbitrarily at x10 magnification, with each imaged area being $4mm^2$. The images were processed using Matlab, and the micropores on the cement surface were recognised based on grey scale thresholds, figure 1. The mean porosity was calculated using the method reported by J Wang et al [5]. The static shear strength was obtained by

$$\sigma = \frac{F}{\pi DL(1-\eta)} \tag{1}$$

Where F is the initial debonding force; D is the rod diameter; L is the internal length of rod within the cement mantle, and η is the porosity of the cement. The mean static shear strength and porosity were then calculated for the five tests carried out for each cement type, with results ranging from 1.89MPa to 4.59MPa. It was evident from figures 2 and 3 that the static shear strength was more dependent on cement type rather than cement viscosity, and there was a tendency for each cement type showing that in general the less the porosity, the larger the static shear strength. Although the results showed greater values than previous research, they were still lower than the typical mean shear stress at the stem cement interface obtained by a finite element model, approximately 5MPa [6], indicating that debonding at this interface was inevitable for a polished stem during in vivo service.

A typical pull out test result displaying the load-displacement plot is shown in figure 4. The plot exhibits originally a linear increase of load with incremental displacement until the initial debonding force is reached. The force then drops to a lower value before appearing to cycle around 1.4kN until the rod is fully pulled out from the cement and the force returns to zero. Large areas of bone cement transfer films were detected on the rod surface, which it was considered may be involved in the cyclical force reading. Based on Hutchings' theory [7], it is assumed that the friction and cyclical force build up began with the "clean" rod trying to move against the cement surface. The interface is strong and the force increases until a transfer film is formed and the cement flows over the cement transfer film, thus causing a drop in the measured force. It is further considered that the cyclical element of the debonding curve is the result of subsequent breakdown of the interface due to transfer film shear followed by reforming and successive breakdown of new transfer films. The total contact area between the rod and cement is diminished gradually, resulting in a decrease of the cyclical force until the rod is pulled out. Figure 5 shows the topography of the cement transfer film detected on the metallic rod surface, measured by a Talysurf CCI 3000 interferometer at x50 magnification. The height of the transfer film was calculated to be about 10μm, using Surfstand software V3.1.

3 FRETTING WEAR SIMULATION

Although fretting wear has been detected on polished femoral stems in retrieval studies, in vitro simulation to reproduce it has seldom been attempted and even then with only limited success [3]. In the present study, a fretting wear simulation was performed in vitro in an Instron Test Machine 1273, using a polished Exeter V40^{TM} femoral stem and Simplex P bone cement. The cement was hand mixed and delivered into a reamed sawbone utilising a syringe to ensure greater penetration into the cancellous structure. The stem was then implanted and the cement cured. Acrulite resin was employed to stabilise this stem-cement-bone system in a steel tube at a position of about 10˚ in adduction and 9˚ in flexion to the stem axis. The load was applied vertically to the femoral head in compression between 0.3kN and 2.3kN in the form of sine wave to simulate joint force in normal activities, the peak value of which is approximately 3 times of average body weight. The simulation was carried out at 3Hz for 5 million cycles uninterruptedly, corresponding to 5 years' wear. Additionally, 9g/l saline solution was utilised to represent synovial fluid in the body. The Exeter V40^{TM} femoral stem was measured with reference to Gruen zones pre and post simulation to detect any evidence of surface changes, using the Talysurf CCI interferometer at x20 magnification. Selected 3D surface parameters, Sq, Sz, Sdq, Ssc and Sdr, were employed to quantitatively assess fretting wear, table 2.

The stem was found to be firmly fixated in the cement mantle when the simulation was finished. After extraction and cleaning with alcohol, the stem showed evidence of fretting wear on all its surfaces, the location of which complied well with clinical studies [2], concentrating mainly on posteromedial and anterolateral zones, figure 6. The selected 3D surface parameters all increased significantly after simulation, indicating that the stem surface had changed a lot. The stem was then cut into pieces, enabling observation using a scanning electron microscope (SEM) JEOL JSM–6060, figure 7(a). Figure 7 (b) shows fretting wear of an explanted Exeter stem, the pitting and dimple characteristics of which are similar to the result of the present simulation. This confirmed that fretting wear was successfully reproduced. Additionally, the sawbone was cut longitudinally into two equal parts to enable investigation of the cement surface, using a Leica stereomicroscope MZ6. There were many macro and micropores present on the cement surface which corresponded well to the undamaged "islands" surrounded by the fretting areas on the stem surface, figure 8. These pores were considered to be formed during cement mixing, delivering and stem implantation process, and have previously been cited as significant contributors to fatigue crack generation, debonding at the stem cement interface, and subsequent failure of cemented THR [8]. It was assumed in this study that the macro and micropores played an important part in initiation and propagation of fretting wear, taking into consideration that the contact between femoral stem and the edge of the pores would facilitate relative micromotion under cyclical loading. The micromotion was prerequisite for fretting wear due mainly to differential stress distribution across the differing thickness of bone cement. Furthermore, it was indicated from a gross inspection that the bone cement was more severely damaged where the surface was in contact with the fretting zones on the femoral stem. Figure 9 displays the topography of "worn" areas and "unworn" areas on the cement surface, which confirmed this concept.

4 CONCLUSIONS

A deep insight into the characteristics at the stem cement interface in cemented THR was gained through a series of pull out tests and an in vitro fretting wear simulation. The static shear strength was compared across seven commercially available bone cements, which, in spite of higher values, were lower than the typical mean shear stress at the stem cement interface. The results were significantly influenced by cement type rather than cement viscosity. In addition, fretting wear was successfully reproduced in vitro which complied well with retrieval investigations. The macro and micropores on the cement surface were considered to contribute significantly to initiate and propagate fretting wear.

REFERENCES

1. Towheed TE, Hochberg MC. Health related quality of life after total hip replacement. Semin Arthritis Rheum1996; 26: 483–491.
2. Howell JR, Blunt LA, Doyle C, Hooper RM, Lee AJ and Ling RS. In vivo surface wear mechanisms of femoral components of cemented total hip arthroplasties: The influence of wear mechanism on clinical outcome. J Arthroplasty 2004; 19: 88–101.
3. Cook JE. Fretting wear of total hip replacement femoral stems. PhD thesis, University of Exeter, Exeter, 1998.
4. Brown L. The use of 3D surface analysis techniques to investigate the wear of matt surface finish femoral stems in total hip replacement. PhD thesis, University of Huddersfield, Huddersfield, 2006.
5. Wang JS, Taylor M, Flivik G and Lidgren L. Factors affecting the static shear strength of the prosthetic stem–bone cement interface. J Mater Sci Mater Med 2003; 14: 55–61.
6. Chang PB, Mann KA and Bartel DL. Cemented femoral stem performance: Effect of proximal bonding, geometry, and neck length. Clin Orthop Relat Res 1998; 355: 57–69.
7. Hutchings IM. Tribology: Friction and wear of engineering materials. London: Edward Arnold; 1992: 51–55.
8. Jasty M, Maloney WJ, Bragdon CR, O'connor DO, Haire T and Harris WH. The initiation of failure in cemented femoral components of hip arthroplasties. J Bone Joint Surg 1991; 73–B: 551–558.

Table1: Relative viscosity and composition of the seven commercial PMMA bone cements

Bone cements	Viscosity	Powder (w/w)	Liquid (w/w)
Cemfix 3	Low	PMMA—87.6; BPO—2.4; BaSO4—10	MMA—84.4; DMPT—2.4; BMA—13.2; HQ—20ppm
Coriplast 3	Low	PMMA—45; PMMA/MA—45; BaSO4—10	MMA—98; DMPT—2; HQ—45ppm
Simplex P	Medium	PMMA—15; PMMA/ST—75; BaSO4—10	MMA—97.4; DMPT—2.6; HQ—60ppm
Simplex P-T	Medium	PMMA—15; PMMA/ST—75; BaSO4—7.5; T—2.5	MMA—97.4; DMPT—2.6; HQ—60ppm
CMW 3	Medium	PMMA—88; BPO—2; BaSO4—10	MMA—97.5; DMPT—2.5; HQ—25ppm
CMW 1	High	PMMA—88.85; BPO—2.05; BaSO4—9.1	MMA—99.18; DMPT—0.82; HQ—25ppm
Palacos R	High	PMMA/MA—84.25 ; BPO—0.75; ZrO2—15; C—200ppm	MMA—97.87; DMPT—2.13; HQ—64ppm; C—267ppm

Note: PMMA—Polymethylmethacrylate; MMA—Methylmethacrylate; BPO—Benzoylperoxide; $BaSO_4$—Barium Sulphate; ZrO2—Zirconium Dioxide; DMPT—N, N-dimethyl-p-toluidine; HQ—Hydroquinone; PMMA/MA—Polymethylmethacrylate-methylacrylate; PMMA/ST—Polymethylmethacrylate-styrene; BMA—Butylmethacrylate; T—Tobramycin; C—Chlorophyll.

Table 2: Selected 3D surface parameters to assess fretting wear

3D parameters	Abbreviation	Explanation
Amplitude parameters	Sq	Root mean square deviation of the topographic surface
	Sz	Height between the tallest peak and deepest valley
Hybrid parameters	Sdq	Root mean square slope of the topographic surface
	Ssc	Arithmetic mean summit curvature of the topographic surface
	Sdr	Developed interface area ratio

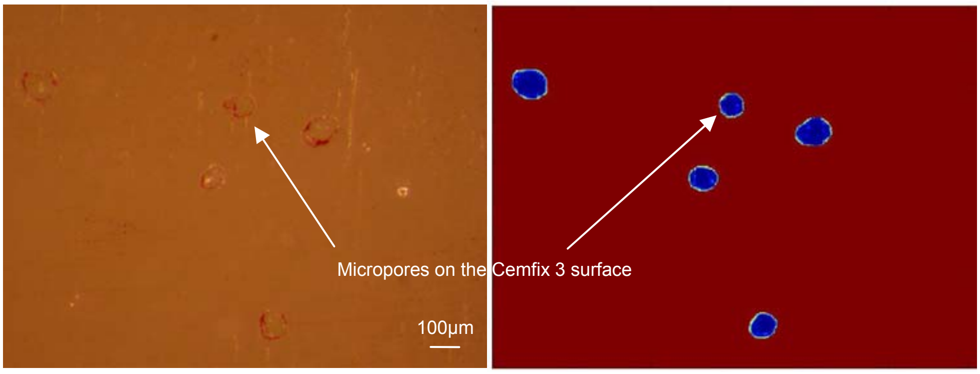

(1a) Original image from Leica microscope (1b) Processed image using Matlab

Figure 1: Detection of micropores

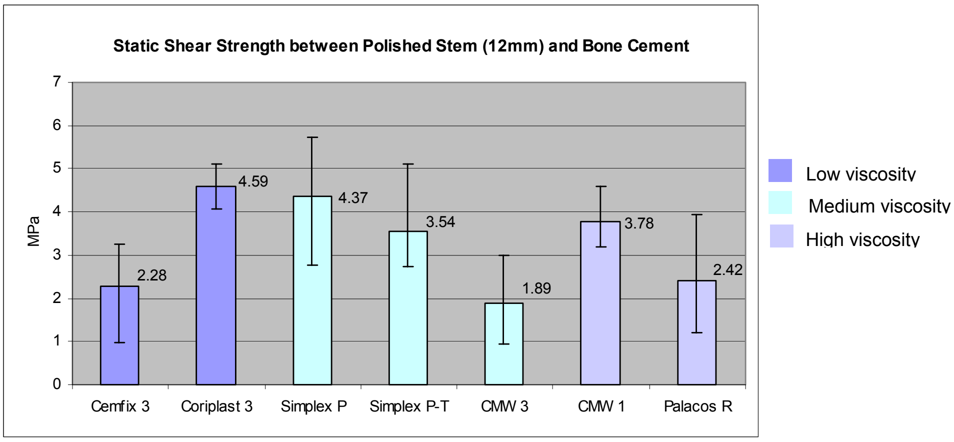

Figure 2: Histogram showing static shear strength at the stem cement interface

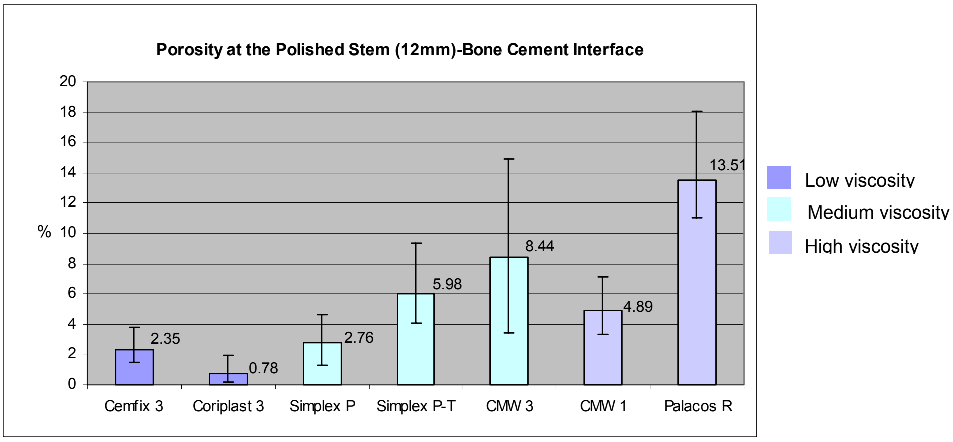

Figure 3: Histogram showing porosity at the stem cement interface

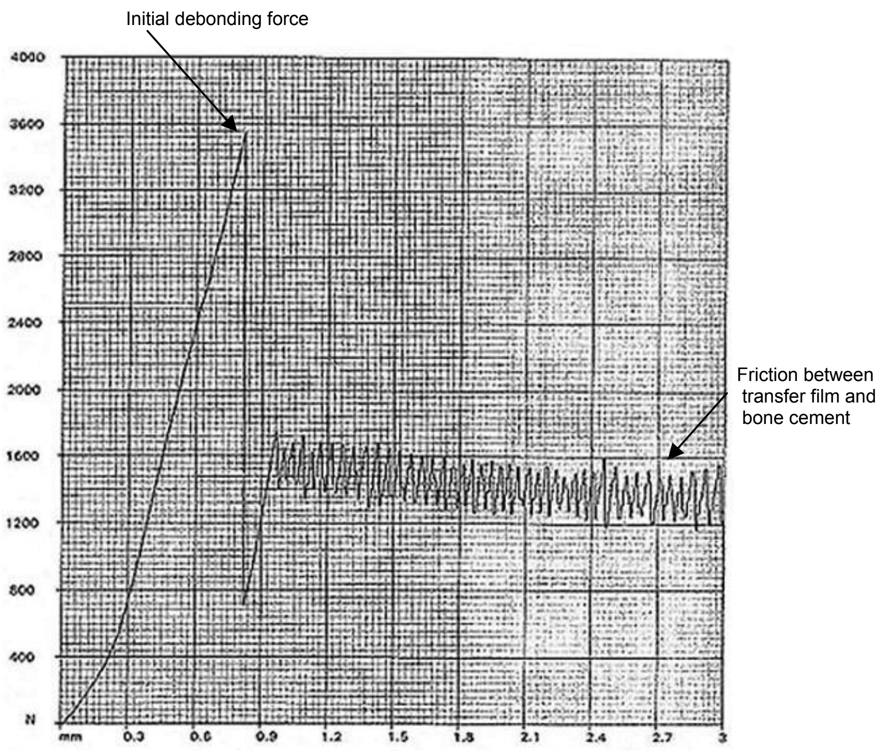

Figure 4: A typical load-displacement plot for CMW 3 bone cement

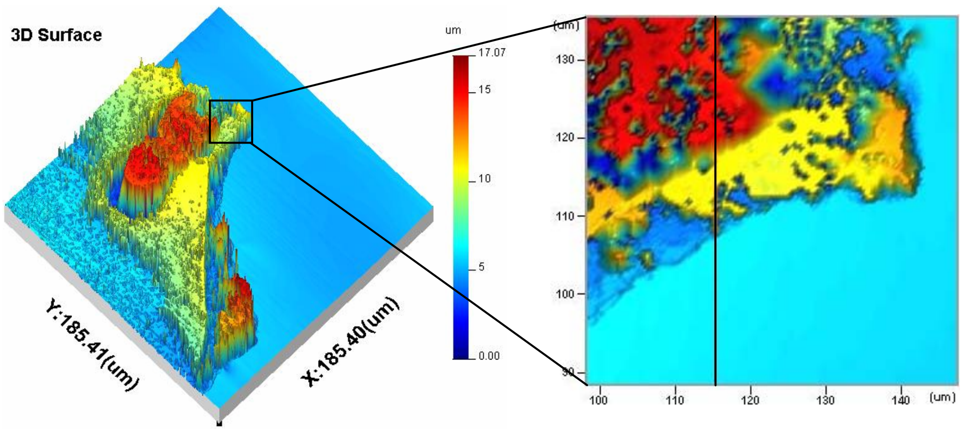

(5a) 3D topography

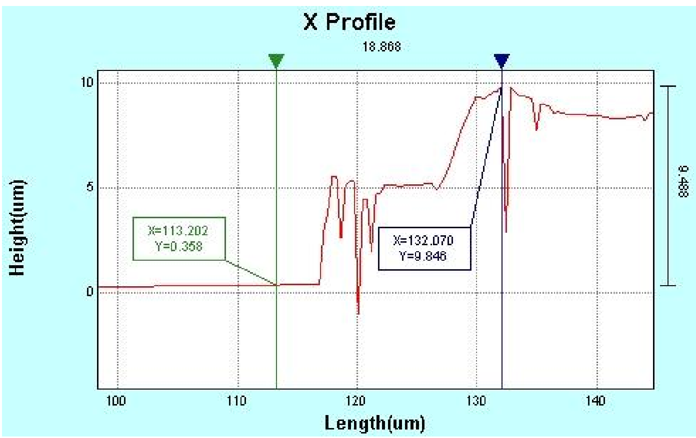

(5b) 2D profile

Figure 5: Transfer film of CMW 3 bone cement on the polished stem surface

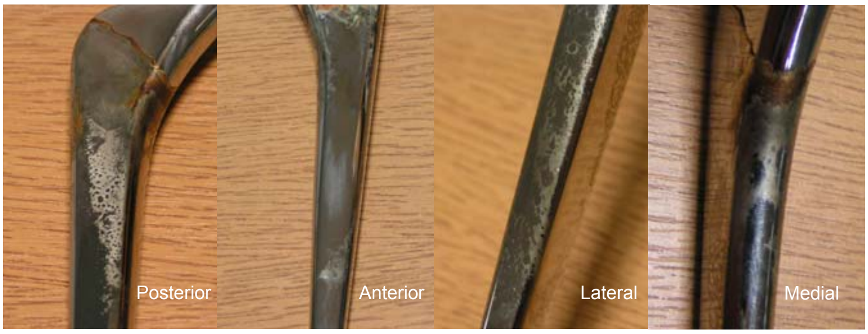

Figure 6: Fretting wear generated on the femoral stem surface

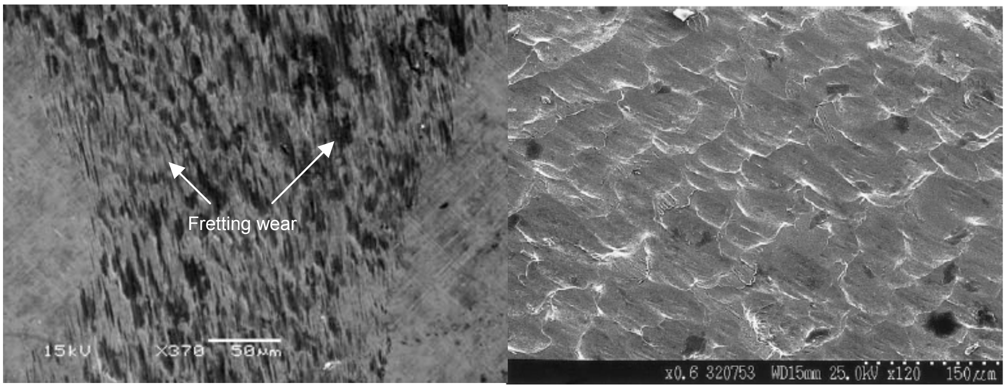

(7a) Fretting wear on the simulated stem

(7b) Fretting wear on the explanted stem

Figure 7: Comparison of fretting wear between simulated and explanted femoral stem

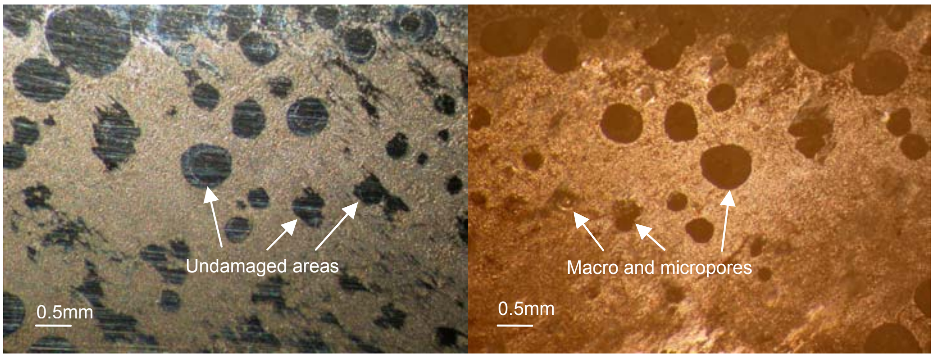

Figure 8: Undamaged areas on the stem surface and corresponding areas on the cement surface

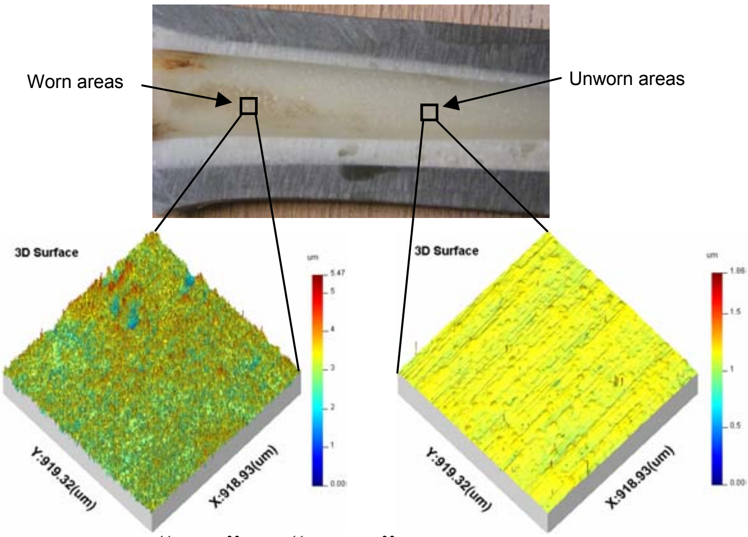

Figure 9: "Worn" and "unworn" areas on the cement surface